Journal of Materials Chemistry A

ROYAL SOCIETY OF CHEMISTRY

PAPER

View Article Online
View Journal | View Issue

Cite this: J. Mater. Chem. A, 2025, 13, 19933

Drive-throughs to driveways: high-strength composites from multi-material post-consumer waste collected from fast food restaurants†

Katelyn M. Derr,[a] Perla Y. Sauceda-Oloño,[a] Ashlyn D. Smith,*[a] Andrew G. Tennyson *[ab] and Rhett C. Smith *[a]

Mixed post-consumer fast food waste poses a formidable challenge for chemical recycling due to its diverse composition of plastics, paper, and remnant foodstuffs. Herein is presented a strategy for kilogram-scale upcycling of such waste into high strength composites. This is accomplished by thiocracking fast food restaurant waste pulp (10 wt%) with sulfur (90 wt%) at 180 °C and 230 °C, giving composites **RWS$_{90}$@180** and **RWS$_{90}$@230**, respectively. These composites display compressive strengths of 12.2–16.3 MPa and flexural strengths of 2.80–5.39 MPa, competitive with common construction materials such as standard building brick (C62 classification) and approaching values for Ordinary Portland Cement (OPC). Both materials exhibit favorable properties under acid challenge (retaining up to 91% of their compressive strength after immersion in 0.5 M H_2SO_4) and show exceptionally low water uptake (<0.5%). Composites **RWS$_{90}$@180** and **RWS$_{90}$@230** also showed low *E* factors, (0.1 and 0, respectively) and low global warming potentials (−0.0450 kg CO_2e per kg and 0.0450 kg CO_2e per kg, respectively). This work highlights an approach to upcycling otherwise problematic mixed-material restaurant waste into durable, corrosion-resistant composites with a low environmental impact.

Received 28th February 2025
Accepted 15th May 2025

DOI: 10.1039/d5ta01674f

rsc.li/materials-a

1. Introduction

Single-use fast food packaging, often heavily soiled by food residues and comprising multiple types of materials (paper, plastic, adhesives, foil liners), remains a difficult target for conventional recycling. The scale of this challenge is enormous: in the United States alone, 11–16.5 million metric tons of food service waste is generated every year,[1] with a substantial fraction (>15%) arising from fast food restaurants.[2] Because this waste stream is a mixture of paper, polystyrene, polypropylene, coatings, adhesives, and food residue, achieving efficient chemical recycling of these comingled components is notoriously complicated.[2] Plastic waste, in particular, degrades slowly and releases microplastics or other pollutants into natural ecosystems.[3–5] As the global consumption of single-use items continues to rise, the need for processes that can upcycle these heterogeneous wastes in a single stage—without requiring extensive sorting—becomes ever more urgent.

In parallel with the challenge of multi-material waste streams, the petrochemical industry generates vast amounts of elemental sulfur as a byproduct of crude oil refining, accruing an estimated 80 million metric tons yearly.[6,7] Transforming this byproduct sulfur into value-added materials is also an important sustainability goal. One established method for sulfur-based polymeric materials is "inverse vulcanization" (Scheme 1A),[8,9] in which thermally activated S–S radical chains react with unsaturated organic substrates to form crosslinked structures.[10–44] Initial studies utilizing sulfur as a majority component to create high sulfur-content materials (HSMs) focused on using modified cellulose,[45,46] plant oils,[42,47–51] and biomass in the form of peanut shells.[52–55] In the case of the reaction of sulfur with peanut shells – comprised of cellulose, lignin, and peanut oil – composite formation occurs *via* tandem transesterification/inverse vulcanization at 180 °C (Scheme 1B).

More recently, we demonstrated that additional S–C bond-forming mechanisms can be employed to address various single source waste plastics through thiocracking.[56,57,61,62] Tandem transesterification/inverse vulcanization routes similar to that shown in Scheme 1B, for example, proved effective in recycling polyethylene terephthalate (PET) waste as well as more complex mixed-material packaging waste containing PET and triglycerides.[59] Polystyrene (as post-consumer foam cups, lids, packaging cubes and plastic silverware) was also successfully converted into high strength composites by thiocracking.[60] The mechanism of S–C bond formation during the thiocracking of polystyrene was investigated in some detail, and several microstructures were identified (Scheme 1C), all resulting from

[a]Department of Chemistry, Clemson University, Clemson, SC, 29634, USA. E-mail: rhett@clemson.edu

[b]Department of Materials Science and Engineering, Clemson University, Clemson, SC, 29634, USA

† Electronic supplementary information (ESI) available. See DOI: https://doi.org/10.1039/d5ta01674f

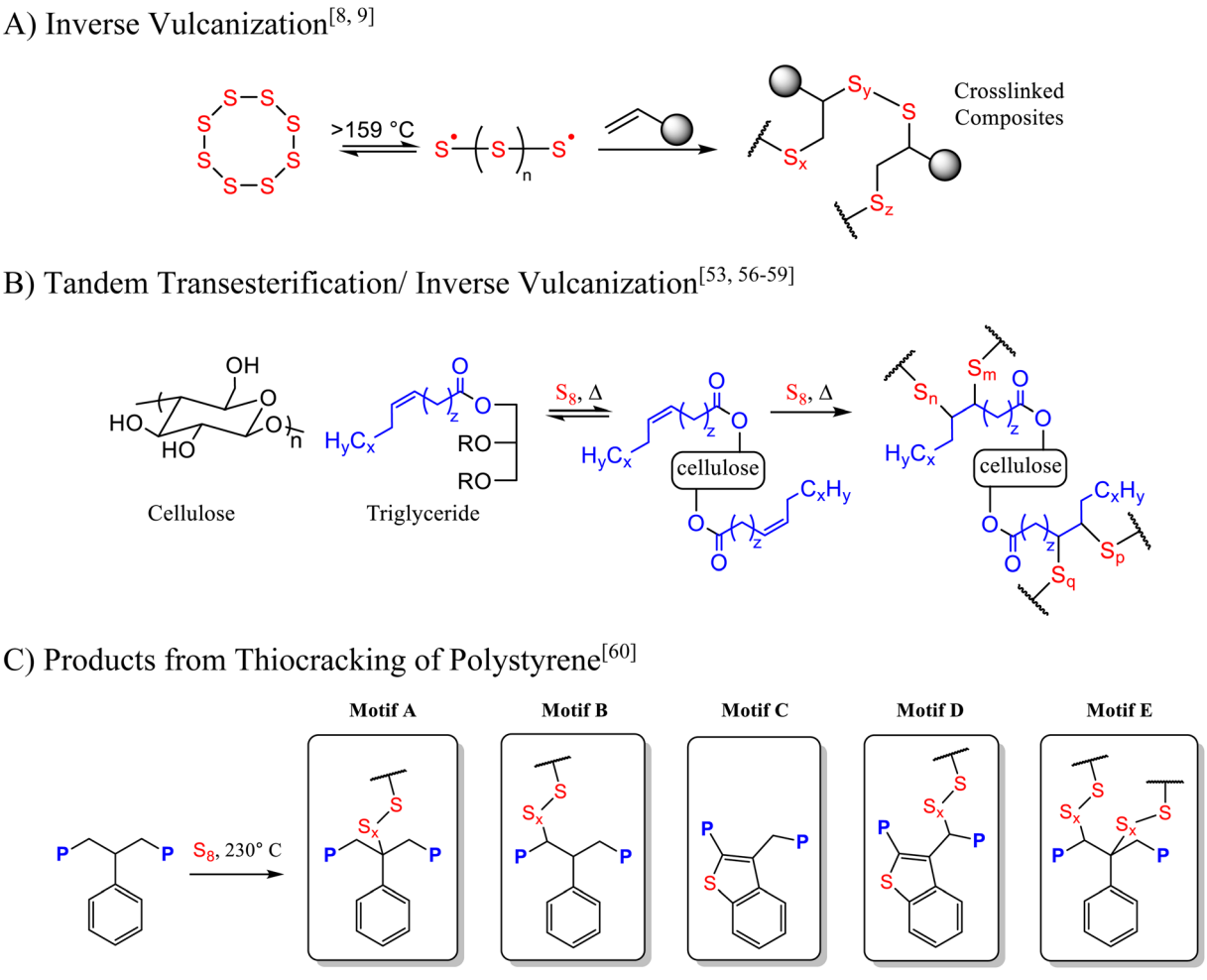

Scheme 1 Crosslinked composites can be made *via* inverse vulcanization of alkenes (A), tandem transesterification/inverse vulcanization of cellulose or lignin and triglycerides (B), or by thiocracking polystyrene with sulfur at 230 °C (C), where P indicates polymer chain attachment).

initial abstraction of benzylic hydrogen atoms from polystyrene by sulfur radicals.

The successful conversion of diverse waste materials to composites through S–C bond-forming chemistry led us to hypothesize that even complex mixed material waste containing plastic, paper, and food waste could be successfully converted to composites by heating with elemental sulfur. Herein we report the effectiveness of thiocracking to convert post-consumer fast food waste (polystyrene cups/lids, straws, wrappers, sandwich boxes, bags, napkins, and food remnants; Fig. 1) into composites in a single synthetic step.

Two reaction temperatures, 180 °C and 230 °C, were investigated to evaluate the extent to which temperature might influence crosslinking through accessible reaction pathways and consequently impact material properties. The resulting materials, **RWS$_{90}$@180** and **RWS$_{90}$@230**, were characterized by mechanical strength testing, thermogravimetric analysis (TGA), differential scanning calorimetry (DSC), mechanical property retention after acid exposure, water uptake, and environmental impact metrics. Each composite exhibits compressive and flexural strengths comparable to or surpassing established construction materials such as C62 building brick and, in some respects, approaches Ordinary Portland Cement (OPC). Scalability of the process was demonstrated by preparing a ~1 kg brick of **RWS$_{90}$@230** having compressional strength capable of supporting a residential vehicle. Not only are these composites prepared entirely from waste materials, but they also showed favorable environmental impact metrics. **RWS$_{90}$@180** has an *E* factor[63] of 0.1 and a negative global warming potential of −0.0450 kg CO_2e per kg, while **RWS$_{90}$@230** has an impressive *E* factor of 0 with a low global warming potential of 0.0450 kg CO_2e per kg. The process's simplicity and excellent sustainability profile underscore the potential of this process for valorizing mixed-material food service waste while simultaneously finding practical uses for stockpiled elemental sulfur.

2. Results and discussion

2.1 Preliminary analysis of multi-material restaurant waste

Post-consumer fast food waste used in this study consisted of cups with lids and straws, sandwich containers (boxes and bags), napkins, straw wrappers, meal bags, and discarded

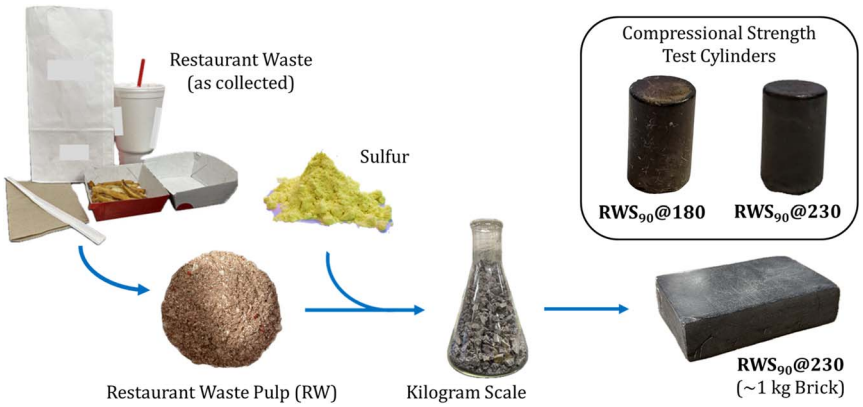

Fig. 1 Fast food waste was collected from fast food restaurants were ground into a fine mixture (**RW**) to be reacted with elemental sulfur to create the high sulfur-content materials **RWS$_{90}$@180** and **RWS$_{90}$@230**.

French fries. The waste was collected directly from tables at source restaurants. Representative waste from one fast food meal was determined to include one cup (polystyrene) complete with the straw (polypropylene) and lid (polystyrene with <5 wt% added polybutadiene), a sandwich container (cardboard box or paper bag-like wrapper), one paper napkin, one paper straw wrapper, a paper meal bag, and 38.8 g of French fries. Less than 5 wt% of the representative restaurant waste was attributable to other sources. Waste from a total of five sample meals was utilized to serve as the organic component in this study. The relative contribution of various components to the mixture was determined (Table 1). The composition reported in Table 1 was determined by manually separating, drying, and weighing the components of five representative fast food meals. French fries used were from the same supply as those for which we previously reported the composition.[64] Cellulose was the primary component of the meal bag, sandwich box/bag, napkin, and straw wrapper, comprising 26.5 wt% of the waste. These components also included minor contributors, such as dyes and adhesives, which were not further quantified. The polystyrene cup and lid comprised another 16.4 wt% of the sample, while the polypropylene straw accounted for 1.07 wt% of the sample. Discarded French fries comprised the largest proportion of the waste, at 56.0 wt%. We previously reported the composition of these fries as 41% water, 33% starch, 23% peanut oil, and 3% other materials such as vitamins and minerals.[55] Preliminary analysis of the components comprising the sample meal was carried out using ^{1}H NMR spectrometry, infrared spectroscopy, thermogravimetric analysis, and differential scanning calorimetry (Fig. S1–S10, S17–S25 and S28–S36†). These data are consistent with the known properties of the constituent components. For example, fries exhibit thermal mass loss below 150 °C due to evaporation of moisture and volatilization of oils, with a broad endothermic peak around 100 °C in the DSC trace.[64] Polystyrene shows a sharp degradation onset near 400 °C in the TGA and a strong endothermic melting transition around 240 °C.[60] Cellulose-based components, including napkins and sandwich wrappers, display a degradation onset at approximately 260 °C, with overlapping moisture loss and exothermic peaks attributed to cellulose depolymerization.[46,53] These features help inform the thermal behavior of the composite precursors and explain some of the degradation patterns seen in the final composite materials (*vide infra*).

Table 1 Mass breakdown of primary chemical components in restaurant fast food waste

Component	Mass	Percent contribution
Cellulose-based materials[a]	87.5 g	25.6%
Polystyrene	56.1 g	16.4%
Polypropylene	3.66 g	1.07%
Starch[b]	64.1 g	18.8%
Peanut oil[b]	44.7 g	13.1%
Water[b]	79.6 g	23.3%
Other[b]	5.80 g	1.70%

[a] Adhesives and dyes in meal bags and sandwich bags are included in the mass of cellulose-based materials. [b] Component contributions made by French fries.

2.2 Preparation of composites

The fast food waste was processed in a blender to produce a fine aggregate restaurant waste pulp (**RW**, Fig. 1). The blended restaurant waste had a particle size range of approximately 0.5–2 mm based on sieve analysis. The bulk density of the dried pulp was determined to be 0.38 g cm^{-3} using volumetric displacement measurements. Processed **RW** (10 wt%) was combined with elemental sulfur (90 wt%) in a pressure flask under an atmosphere of dry nitrogen gas and then heated at 180 °C or 230 °C for 24 hours to give **RWS$_{90}$@180** or **RWS$_{90}$@230**, respectively. Visually, **RWS$_{90}$@180** was a dark brown solid containing fine aggregates. When handled, this material was relatively brittle. In contrast, **RWS$_{90}$@230** was a black solid that was much more resistant to breakage when handled. The apparent difference in mechanical strength may be attributed to the higher degree of crosslinking anticipated in **RWS$_{90}$@230** compared to that in **RWS$_{90}$@180**; prior studies indicated that minimal reaction of polystyrene (comprising

16.4 wt% of **RW**) occurs at 180 °C, whereas extensive reactivity (*i.e.*, Scheme 1C) is observed at 230 °C.[60] Further evidence for crosslink density dependence on temperature was also derived from thermal, morphological and mechanical tests (*vide infra*). Both composites were remeltable and could be readily poured into molds to prepare shapes for mechanical testing or applications (Fig. 1). The viability of the process for scaleup to the kilogram scale was further validated by preparing a brick (~1 kg) of **RWS$_{90}$@230**.

FT-IR spectroscopy is often a useful technique providing evidence of S–C bond-formation following the reaction of organics with elemental sulfur. However, it is sometimes difficult to discern the already weak S–C stretch in spectra for HSMs comprising 90 wt% sulfur. For this reason, HSMs are often depolymerized using $LiAlH_4$, which breaks S–S bonds and converts the S–C crosslink points to thiols.[9] This significantly decreases the presence of sulfur in the material while retaining S–C bonds for analysis by IR spectroscopy with an improved signal-to-noise ratio. Depolymerization of **RWS$_{90}$@180** and **RWS$_{90}$@230** by a modification of the procedure reported by Pyun[9] gave **d-RWS$_{90}$@180** and **d-RWS$_{90}$@230**, respectively. Evidence of S–C bonds was observed as a broad stretch at 697 cm^{-1} in the depolymerized materials (Fig. 2).

Elemental homogeneity was confirmed through scanning electron microscopy with elemental mapping by energy dispersive X-ray (SEM/EDX). These images showed little evidence of phase separation on the surface of the material on a 100 μm scale with an even distribution of carbon, oxygen, and sulfur throughout both **RWS$_{90}$@180** and **RWS$_{90}$@230** (Fig. S15 and S16†). Another measure of elemental distribution is the extent to which added sulfur is present as oligo- or poly-sulfur catenates covalently bound to organic comonomers *versus* being present as physically entrapped sulfur species known as "dark sulfur".[65] The amount of dark sulfur in **RWS$_{90}$@180** and **RWS$_{90}$@230** was quantified using a recently published method,[66] wherein the dark sulfur in HSMs is extracted into ethyl acetate and quantified using UV-vis spectroscopy. **RWS$_{90}$@180** and **RWS$_{90}$@230** were determined to contain 64 wt% and 52 wt% dark sulfur, respectively. The greater proportion of dark sulfur in **RWS$_{90}$@180** is consistent with less crosslinking at the lower reaction temperature. The dark sulfur contents of **RWS$_{90}$@180** and **RWS$_{90}$@230** are also similar to those of HSMs prepared from thiocracking of 10 wt% polystyrene with 90 wt% sulfur at 230 °C, which contained 40–54 wt% dark sulfur.[60]

2.3 Thermal and morphological properties of composites

Thermogravimetric analysis (TGA) of **RWS$_{90}$@180** and **RWS$_{90}$@230** (Table 2 and Fig. S26, S27†) were performed to evaluate their thermal stability. The decomposition temperature (T_d, defined as the temperature at which 5% mass loss has occurred) was determined to be 200 °C for **RWS$_{90}$@180** and 217 °C for **RWS$_{90}$@230**, compared to 229 °C for elemental *cyclo*-S_8. Mass loss in these materials is attributed to the sublimation of sulfur, both from dark sulfur and from sulfur formed during the thermal breakdown of polysulfur crosslinking chains. Smaller mass loss steps at higher temperatures are likely attributable to the decomposition of cellulose derivatives and organosulfur aryls formed from polystyrene-derived domains.

Differential scanning calorimetry (DSC) measurements (Table 2 and Fig. S37, S38†) further elucidated the thermomorphological properties of the composites. Both **RWS$_{90}$@180** and **RWS$_{90}$@230** exhibited a prominent melting event at 118 °C and 117 °C, respectively, consistent with the melting of orthorhombic sulfur. **RWS$_{90}$@230** exhibited a single cold crystallization peak at 23 °C and did not display an observable glass transition temperature (T_g). In contrast, **RWS$_{90}$@180** showed two cold crystallization events at −10 °C and 36 °C and a glass transition at −38 °C. The T_g in **RWS$_{90}$@180** is attributable to polymeric sulfur domains, confirming the presence of relatively long sulfur catenates in this material. Calculations based on melting and cold crystallization enthalpies indicate that **RWS$_{90}$@180** has a percent crystallinity of 72–77%, while **RWS$_{90}$@230** exhibits a significantly lower crystallinity of 21%. Both the absence of a T_g in the range typically observed for

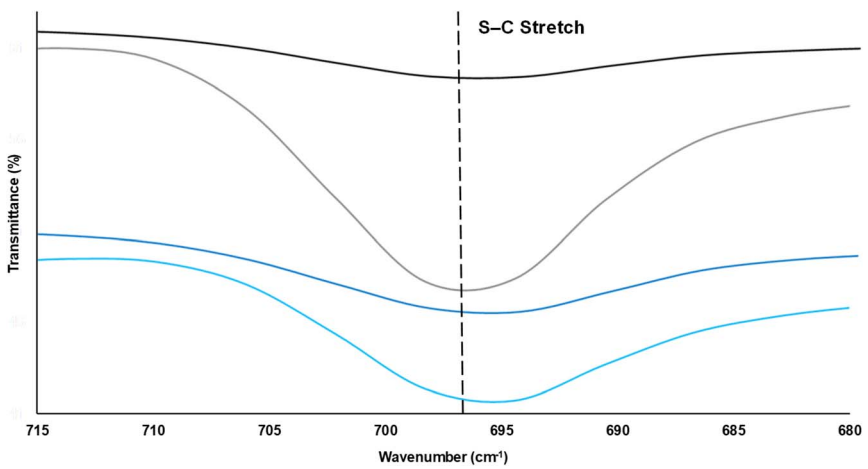

Fig. 2 FT-IR spectra for RWS$_{90}$@180 (black trace), d-RWS$_{90}$@180 (gray trace), RWS$_{90}$@230 (dark blue trace), and d-RWS$_{90}$@230 (light blue trace) demonstrate the formation of S–C bonds evident by the band at 697 cm^{-1}. ESI Fig. S11–S14† provide the full spectra for these materials.

Table 2 Thermal and morphological properties of restaurant waste and sulfur composites **RWS$_{90}$@180** and **RWS$_{90}$@230** compared to elemental sulfur

Material	T_d[a] °C	T_m[b] °C	T_g[c] °C	ΔH_m J g^{-1}	ΔH_{cc} J g^{-1}	Percent crystallinity[d]
RWS$_{90}$@180	200	118	−38, −11	38	−3, −5	72–77
RWS$_{90}$@230	217	117	NA	33	−23	21
S_8	229	118	NA	44.8	NA	100

[a] Temperature at which 5% mass loss is observed. [b] Temperature at the peak maximum of the endothermic melting from the third heating cycle. [c] Glass transition temperature. [d] Reduction of percent crystallinity of each sample calculated with respect to sulfur (normalized to 100%).

HSMs containing longer sulfur catenates and a lower observed crystallinity in **RWS$_{90}$@230** are consistent with the anticipated higher degree of crosslinking and concomitantly shorter sulfur catenates at the higher reaction temperature.

2.4 Mechanical properties and microstructures

Cylinders suitable for compressive strength analysis were prepared by melting each composite and pouring the molten materials into silicon molds. All compressive strength samples were allowed to sit for 96 h at room temperature before analysis to allow for post-reaction crosslinking, following standard conventions for other HSMs.[45] The compressive strength of **RWS$_{90}$@180** was determined to be 12.2 ± 0.8 MPa, and **RWS$_{90}$@230** was found to have a compressive strength of 16.3 ± 0.6 MPa (Fig. S39 and S40†). These values are competitive with the minimum requirements for OPC in building foundations[67] and 142% and 190% stronger than C62 brick, respectively. These composites made from multi-component restaurant waste have lower compressive strengths compared to other HSMs such as **APS$_{95}$** (made from allylated peanut shells and sulfur)[52] **H$_0$O$_{10}$S$_{90}$** (made from peanut oil, peanut shells, and sulfur) and **WFFS$_{90}$** (made from French fries and sulfur).[55] However, the restaurant waste derived composites have comparable compressive strengths to those of HSMs made from polystyrene[60] (more details on the composition of these composites are provided in the footnote to Table 3, and a visual synopsis of these data is provide in Fig. 3). A qualitative compressive strength test was also performed wherein a ∼1 kg brick of **RWS$_{90}$@230** was prepared. The brick's compressive strength was demonstrated by holding the weight of a 4-door sedan without any obvious physical deformation or damage to the brick. The improved mechanical properties of **RWS$_{90}$@230** (16.3 ± 0.6 MPa compressive, 5.39 ± 0.81 MPa flexural) compared to **RWS$_{90}$@180** are attributed to greater crosslink density, as evidenced by a 12% lower dark sulfur content and a moderately higher decomposition temperature (217 °C *versus* 200 °C). Significantly reduced crystallinity (21% *versus* 72–77%) of the sample made at 230 °C *versus* 180 °C also supports a denser, more amorphous network structure consistent with enhanced crosslinking. The denser crosslinking is also consistent with the report that polystyrene (comprising 16.4% of organics in restaurant waste) is not effectively crosslinked upon heating with sulfur at 180 °C, but is at 230 °C.[60]

While mineral-based building materials like OPC are used in various construction applications, they exhibit some weaknesses, especially when exposed to acid or water. Sulfur's acid-resistance and hydrophobic properties can be imbued to the resulting HSMs. After submersion in 0.5 M H_2SO_4 for 24 h, **RWS$_{90}$@180** and **RWS$_{90}$@230** retained 67% and 91% of their strength, respectively. Under exposure to the same conditions, mineral-based legacy materials such as OPC dissolve. A main point of failure for OPC comes from the expansion and contraction of the material due to absorbed water freezing and thawing within the material, which can cause significant cracks. OPC can absorb up to 28% of its weight in water; conversely, following submersion in water for 24 h, **RWS$_{90}$@180** absorbs

Table 3 Mechanical properties of **RWS$_{90}$@180** and **RWS$_{90}$@230** compared to other high sulfur-content materials and commercial building materials

Material	Compressive strength (MPa)	After acid (MPa)	Strength retained (%)	Flexural strength (MPa)
RWS$_{90}$@180	12.2 ± 0.8	8.2 ± 1.0	67%	2.80 ± 0.42
RWS$_{90}$@230	16.3 ± 0.6	14.9 ± 0.6	91%	5.39 ± 0.81
APS$_{95}$[a]	35.7	ND	ND	4.8
H$_0$O$_{10}$S$_{90}$[b]	25.9	ND	ND	ND
WFFS$_{90}$[c]	33.8	ND	ND	ND
PSC$_{90}$[d]	7.7	ND	ND	2.15
PSL$_{90}$[e]	12.8	ND	ND	1.92
C62 brick[f]	8.6	ND	ND	ND
OPC	17	ND	ND	3.7

[a] Composite of allylated peanut shells (5 wt%) and sulfur (95 wt%).[52] [b] Composite of peanut oil (10 wt%) and sulfur (90 wt%).[55] [c] Composite of French fries (10 wt%) and sulfur (90 wt%).[55] [d] Composite of a polystyrene cup (10 wt%) and sulfur (90 wt%).[60] [e] Composite of a polystyrene lid (10 wt%) and sulfur (90 wt%).[60] [f] Brick classification C62 for building brick with normal weathering.[68]

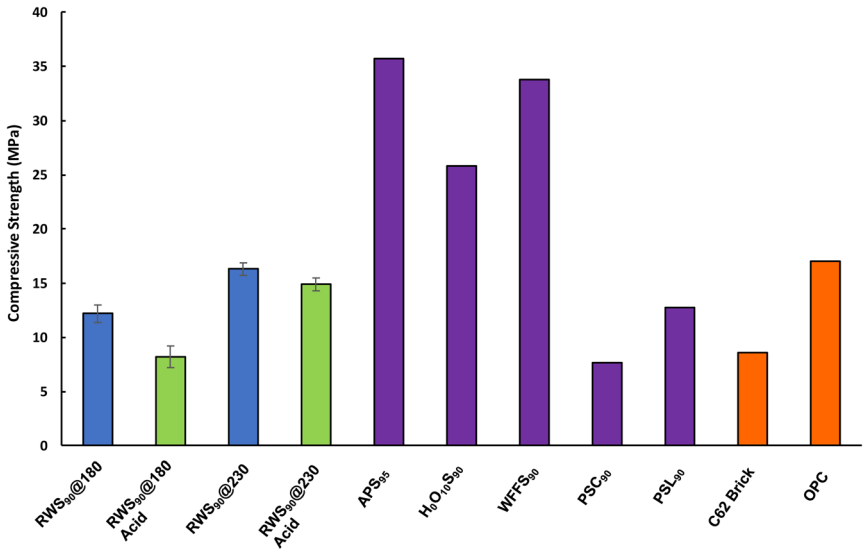

Fig. 3 Compressive strengths of RWS_{90}@180 and RWS_{90}@230 compared to other high sulfur-content materials and commercial building materials.

only 0.45% of its weight in water, and **RWS_{90}@230** exhibits a remarkably low 0.13% uptake of water.

Rectangular prisms for flexural strength determination by dynamic mechanical analysis (DMA, Table 3 and Fig. S41, S42†) were prepared by melting each material and pouring into molds. All samples were milled to a thickness of 1.5 mm and allowed to sit for 96 h at room temperature before testing. **RWS_{90}@180** was determined to have a flexural strength of 2.80 ± 0.42 MPa, similar to other HSMs prepared from polystyrene (**PSC_{90}** and **PSL_{90}** in Table 3). **RWS_{90}@230** was found to have a flexural strength of 5.39 ± 0.81 MPa which exceeds the average value of OPC's flexural strength of 3.7 MPa.

The successful incorporation of sulfur and organic components into an insoluble crosslinked composite, along with literature precedent for the reactivity of various components found in the fast food restaurant waste, allows us to propose the microstructural features of the restaurant waste-derived composites **RWS_{90}@*T*** (Scheme 2). Prior studies establish S–C bond formation *via* inverse vulcanization (Scheme 1A) of plant oils such as the peanut oil in the restaurant waste,[42,47–51] which takes place in tandem with transesterification in the presence of cellulose and starch (Scheme 1B).[53,56–59] Polystyrene reacts with sulfur to form structural motifs A–E (Scheme 1C).[60] All of these mechanisms are expected to occur when elemental sulfur reacts with the complex mixture of materials found in fast food restaurant waste to give structures such as those shown in Scheme 2.

2.5 Environmental impact

To fully assess the viability of **RWS_{90}@180** and **RWS_{90}@230** to serve as a replacement for mineral-based legacy materials such as OPC, it is essential to analyze the material's environmental impact. One metric that can help provide insight into the environmental impact is the *E* factor,[63] which compares the

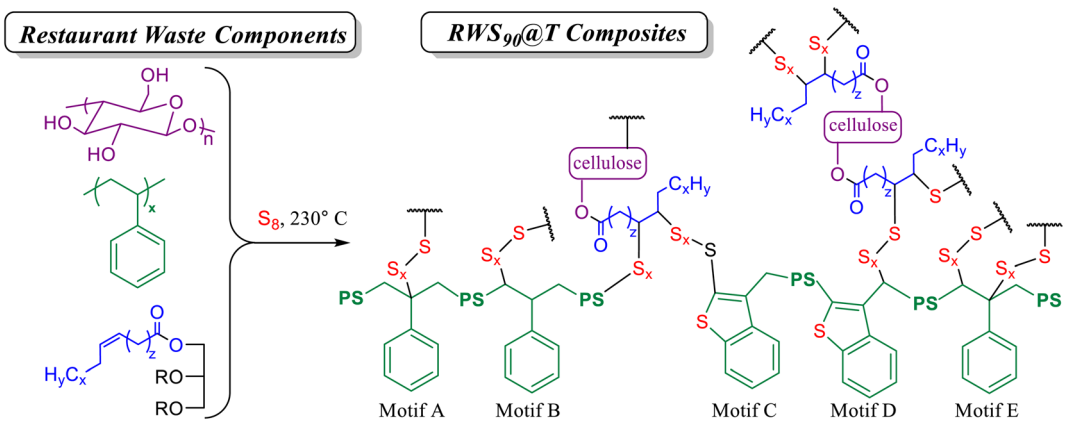

Scheme 2 Representative structural features of composites RWS_{90}@*T*, where PS indicated polystyrene chains, which will be further crosslinked at other positions along the chain. Polystyrene-derived motifs A–E are as based on our published study,[60] as shown in Scheme 1C.

amount of waste produced *versus* the amount of useful products created. A lower E factor correlates to less waste generated, whereas a higher E factor reflects a material that produces a greater amount of waste. For **RWS$_{90}$@180** and **RWS$_{90}$@230**, the E factor was calculated based on the masses in Table 1; each part of the waste was included in the organic component in the preparation of the materials. Thus, the only waste comes from mass loss experienced during the reaction. The following calculations reflect the values had the total amount of waste collected been converted to HSMs:

$$E\ \text{factor}_{\mathbf{RWS_{90}@180}} = \frac{\text{waste}}{\text{useful product}} = \frac{\text{mass loss from sublimed sulfur and gas evolution}}{\text{restaurant waste} + \text{sulfur}} = \frac{341\ \text{g}}{341\ \text{g} + 3069\ \text{g}} = 0.1$$

$$E\ \text{factor}_{\mathbf{RWS_{90}@230}} = \frac{\text{waste}}{\text{useful product}} = \frac{\text{mass loss from sublimed sulfur and gas evolution}}{\text{restaurant waste} + \text{sulfur}} = \frac{0\ \text{g}}{341\ \text{g} + 3069\ \text{g}} = 0$$

The composite **RWS$_{90}$@180** has an E factor of 0.1, whereas **RWS$_{90}$@230** has an impressive E factor of 0, as there was no waste in this process. These values are remarkably lower compared to many other commercial materials such as bulk commercial chemicals which can have E factors ranging from less than 1 to greater than 50,[69,70] and OPC which has an E factor of 1.4.[69]

While the E factor provides insight into the environmental impact based on mass/atom balance, it does not account for energy consumption or emissions. To gain a more complete picture of the environmental impact of these materials, the global warming potential estimates the kilograms of carbon dioxide emitted per kilogram of useful material produced. For **RWS$_{90}$@180**, the global warming potential was determined to be −0.00450 kg CO_2e per kg whereas the global warming potential for **RWS$_{90}$@230** was determined to be +0.00450 kg CO_2e per kg (the full scope and calculations can be found in the ESI†). Compared to the global warming potential of OPC (+1.0 kg CO_2e per kg), whose carbon dioxide emissions account for roughly 8% of CO_2 production, the values found for the **RW**–sulfur composites are far lower.[71]

3. Conclusions

This study demonstrates a noteworthy new approach for upcycling heterogeneous fast-food waste into high strength, sulfur-based composites *via* a one-pot thiocracking process. By employing a mixture of processed restaurant waste pulp (10 wt%) with elemental sulfur (90 wt%) at two reaction temperatures (180 °C and 230 °C), composites **RWS$_{90}$@180** and **RWS$_{90}$@230** were synthesized. These composites exhibit competitive mechanical properties relative to conventional construction materials. Notably, the composite prepared at 230 °C shows enhanced compressive (16.3 ± 0.6 MPa) and flexural strengths (5.39 ± 0.81 MPa), which can be attributed to a higher degree of crosslinking and shorter sulfur catenate lengths, as well as reduced dark sulfur content. These improvements are further reflected in the superior resistance of **RWS$_{90}$@230** to acid challenge and its remarkably low water uptake.[72–87]

Importantly, the scalability of the process was validated by preparing a ∼1 kg brick of **RWS$_{90}$@230**, underscoring the method's potential for industrial application. Additionally, the environmental impact assessments reveal exceptionally low E factors (0.1 for **RWS$_{90}$@180** and 0 for **RWS$_{90}$@230**) and favorable global warming potential metrics, highlighting the minimal waste generation and reduced CO_2 emissions associated with the process. This work not only provides a practical avenue for valorizing multi-material post-consumer waste but also offers a scalable route for transforming an abundant industrial byproduct, elemental sulfur, into value-added, durable construction materials.

Although the composites described here comprise only 10 wt% fast food waste, this method represents a scalable strategy for valorizing complex multi-material post-consumer waste streams and may contribute to reducing petroleum use in applications such as asphalt, for which sulfur-based alternatives have been previously explored.

Quantitative adhesion and wettability characterization (*e.g.*, lap shear and contact angle measurements) are currently underway. Future studies will also aim at further optimizing reaction parameters and broadening the feedstock scope are underway to extend the applicability of this approach.

4. Experimental section

4.1 General considerations

A Blendtec Total blender was used to blend the restaurant waste used in this study.

Proton NMR spectra were acquired on a Bruker NEO-300 MHz at room temperature, and data was processed with MestReNova x64-14.3-30573 software. All spectra reported were calibrated to the residual solvent peak from deuterated chloroform.

Fourier transform infrared spectra were obtained using a Shimadzu IR Affinity-1S instrument with an ATR attachment operating over 400–4000 cm^{-1} at ambient temperature.

UV-vis data was collected on an Agilent Technologies Cary 60 UV-Vis using Simple Reads software. The data was collected at 275 nm.

SEM and EDX were acquired on a Schottky Field Emission Scanning Electron Microscope SU5000 operating in variable pressure mode with an accelerating voltage of 15 keV.

Thermogravimetric analysis (TGA) data were recorded on a TA SDT Q600 instrument over the range 25 to 800 °C, with a heating rate of 10 °C min^{-1} under a flow of N_2 (20 mL min^{-1}).

DSC data were acquired (Mettler Toledo DSC 3 STARe System) over the range −60 to 140 °C with a heating rate of 10 °C min^{-1} under a flow of N_2 (200 mL min^{-1}). Each DSC measurement was carried out over three heat-cool cycles.

For percent crystallinity calculations, T_m, ΔH_m and ΔH_{cc}, the data was taken from the third heat/cool cycle. Melting enthalpies and cold crystallization enthalpies were calculated using DSC data. The reduction of the percent crystallinity of the composite **RWS$_{90}$@180** and **RWS$_{90}$@230** with respect to sulfur was calculated using the following equation.

$$\Delta\chi_c = 1 - \left\{\frac{\Delta H_{m(\mathbf{RWS_{90}@180\ or\ 230})} - \Delta H_{cc(\mathbf{RWS_{90}@180\ or\ 230})}}{\Delta H_{m(S)} - \Delta H_{cc(S)}}\right\} \times 100\%$$

$\Delta\chi_c$ – change of percentage crystallinity with respect to sulfur, $\Delta H_{m(\mathbf{RWS_{90}@180\ or\ 230})}$ – melting enthalpy of composite materials (**RWS$_{90}$@180** or **RWS$_{90}$@230**), $\Delta H_{cc(\mathbf{RWS_{90}@180\ or\ 230})}$ – cold crystallization enthalpy of composite materials, $\Delta H_{m(S)}$ – melting enthalpy of sulfur, $\Delta H_{cc(S)}$ – cold crystallization enthalpy of sulfur.

Compressional analysis was performed on a Mark-10 ES30 test stand equipped with a M3-200 force gauge (1 kN maximum force with ±1 N resolution) with an applied force rate of 3–4 N s^{-1}. Compression cylinders were cast from silicone resin molds (Smooth-On Oomoo® 25 tin-cure) with diameters of approximately 6 mm and heights of approximately 10 mm. Samples were manually sanded to ensure uniform dimensions and measured with a digital caliper with ±0.01 mm resolution. Compressional analysis was performed in triplicate, and the results were averaged.

Flexural strength analysis was performed using a Mettler Toledo DMA 1 STARe System in single cantilever mode. The samples were cast from silicone resin molds (Smooth-On Oomoo® 30 tin-curve). The sample dimensions were approximately 1.5 × 10 × 23 mm. Flexural analysis was performed in triplicate and the results were averaged. The clamping force was 1 cN m.

4.2 Materials, methods, and safe handling warning

Sulfur powder (99.5%) was purchased from Alfa Aesar. Post-consumer restaurant waste (packaging and French fries) was collected from local chain restaurants on the day of disposal by customers. Post-consumer French fries were produced from Idaho potatoes produced in Idaho Falls, Idaho, USA, in the 2023 growing season. Composites were allowed to stand at room temperature for 4 days prior to mechanical testing.

CAUTION: Heating elemental sulfur with organics can consequently result in H_2S or other gas formation. Such gases can be corrosive, foul-smelling, and toxic. Temperature must be cautiously controlled in order to prevent thermal spikes, contributing to the potential for H_2S or other gas evolution. Rapid stirring shortened heating times, and very slow addition of reagents can help avoid unforeseen temperature spikes.

4.2.1 Preparation of restaurant food waste (RW). Post-consumer restaurant food packaging waste and waste French fries (**RW**) were collected on the day of disposal. The mass of each component was recorded to allow for the calculation of each component's contribution to the overall mass of ground **RW** (Table 1). Each component was analyzed by FT-IR spectroscopy (Fig. S2–S10†), TGA (Fig. S17–S25†), and DSC (Fig. S28–S36†). The collected **RW** was placed in the blender in several batches and processed for several minutes to give a fine aggregate that was even mixed to serve as the organic component in the preparation of **RWS$_{90}$@180** and **RWS$_{90}$@230**.

4.2.2 Synthesis of RWS$_{90}$@180. To a 500 mL round bottom pressure flask equipped with a magnetic stir bar was added 54.0 g of elemental sulfur and 6.07 g of **RW**. The flask was then sealed with a Teflon screw cap equipped with a Viton O-ring under an atmosphere for dry nitrogen. The flask was removed from the glovebox and transferred to an oil bath where it was heated at 180 °C for 24 h. Upon cooling to room temperature, 54 g of a dark brown solid was recovered. Elem. anal. calc'd: C 5–10, H 0–5, S 90.0; found: C 1.05, H 0.0, S 98.53.

4.2.3 Synthesis of RWS$_{90}$@230. To a 500 mL round bottom pressure flask equipped with a magnetic stir bar was added 54.0 g of elemental sulfur and 6.06 g of **RW**. The flask was then sealed with a Teflon screw cap equipped with a Viton O-ring under an atmosphere for dry nitrogen. The flask was removed from the glovebox and transferred to an oil bath where it was heated at 230 °C for 24 h. Upon removal from heat, the reaction exhibited no gas evolution upon the vessel being opened to air. This reaction yielded 60 g of a black rigid material with fine aggregate visible throughout. Elem. anal. calc'd: C 5–10, H 0–5, S 90.0; found: C 6.25, H 0.30, S 89.48.

4.2.4 Depolymerization of RWS$_{90}$@180. To a vial equipped with a magnetic stir bar was added 100.4 mg of finely ground **RWS$_{90}$@180**. The vial was transferred to an inert atmosphere where 173.5 mg $LiAlH_4$ was added. The mixture was suspended in 7 mL of anhydrous toluene and the vial secured with a rubber septum wired in place. The mixture was allowed to stir for 24 h at room temperature. After the allotted time the vial was removed and connected to a Schlenk line under constant flow of N_2. The vial was placed in an ice bath and slowly quenched by addition the of 5% (v/v) HCl : ethanol until there was no more

evolution of H_2 gas. The mixture was filtered and washed with DI H_2O (pH = 5) and the organic layer separated and the solvent removed to yield 7 mg of a brown crystalline solid.

4.2.5 Depolymerization of RWS_{90}@230. To a vial equipped with a magnetic stir bar was added 101.5 mg of finely ground **RWS_{90}@230**. The vial was transferred to an inert atmosphere where 173.3 mg $LiAlH_4$ was added. The mixture was suspended in 7 mL of anhydrous toluene and the vial secured with a rubber septum wired in place. The mixture was allowed to stir for 24 h at room temperature. After the allotted time the vial was removed and connected to a Schlenk line under constant flow of N_2. The vial was placed in an ice bath and slowly quenched by addition the of 5% (v/v) HCl : ethanol until there was no more evolution of H_2 gas. The mixture was filtered and washed with DI H_2O (pH = 5) and the organic layer separated and the solvent removed to yield 7 mg of a tan crystalline solid.

4.2.6 Determination of dark sulfur content in RWS_{90}@180. To a 250 mL volumetric flask was added 7.8 mg **RWS_{90}@180** (weighed with a microbalance) and approximately 230 mL ethyl acetate. The mixture was allowed to stir for 30 min after which the solution was diluted to 250 mL with ethyl acetate. 3 mL of this solution was transferred to a cuvette and 3 mL of pure ethyl acetate was transferred to a separate cuvette to serve as a blank. Data was collected at 275 nm and dark sulfur content was calculated from a calibration curve having the equation $y = 36.124x + 0.012$ ($R^2 = 0.9967$), where y is the absorbance and x is the concentration of sulfur in mg mL^{-1}.

4.2.7 Determination of dark sulfur content in RWS_{90}@230. To a 250 mL volumetric flask was added 7.7 mg **RWS_{90}@230** (weighed with a microbalance) and approximately 230 mL ethyl acetate. The mixture was allowed to stir for 30 min after which the solution was diluted to 250 mL with ethyl acetate. 3 mL of this solution was transferred to a cuvette and 3 mL of pure ethyl acetate was transferred to a separate cuvette to serve as a blank. Data was collected at 275 nm and dark sulfur content was calculated from a calibration curve having the equation $y = 36.124x + 0.012$ ($R^2 = 0.9967$), where y is the absorbance and x is the concentration of sulfur in mg mL^{-1}.

4.2.8 Mechanical strength sample preparation. Cylinders with diameters of approximately 6 mm and heights of approximately 10 mm, appropriate for compressive strength measurements, were prepared by melting the composite at 160 °C, then slowly and carefully pouring it into molds and allowing the material to solidify. Samples were stored at room temperature for 4 d prior to strength measurements. The samples were sanded to remove flack and measured with a digital caliper with ±0.01 mm resolution. Prisms with widths of approximately 10 mm, lengths of approximately 10 mm and thicknesses of approximately 1.5 mm, appropriate for flexural strength measurements, were prepared by melting the composite at 160 °C, then slowly and carefully pouring it into molds and allowing the material to solidify. Samples were stored at room temperature for 4 d prior to strength measurements. The samples were sanded to remove flack and measured with a digital caliper with ±0.01 mm resolution.

Data availability

The data supporting this article have been included as part of the ESI.†

Conflicts of interest

There are no conflicts to declare.

Acknowledgements

This research was funded by The National Science Foundation grant number CHE-2203669 to RCS and ACREC grant to RCS and ADS. The author primarily responsible for particular CRediT roles are provided here. K. M. D.: data curation, formal analysis, investigation, validation, writing – original draft. P. Y. S.-O.: supervision. A. D. S.: writing – review and editing, funding acquisition. A. G. T.: resources, supervision. R. C. S.: conceptualization, methodology, resources, supervision, funding acquisition, writing – original draft, review and editing.

References

1 *Trash in America*, Environment America Research & Policy Center, 2021, p. 2024.
2 *Fast Food's Contribution to Food Waste*, Skipshapiro Enterprises, 2024, p. 2024.
3 J. Jeong and J. Choi, *Chemosphere*, 2019, **231**, 249.
4 M. Cole, P. Lindeque, C. Halsband and T. S. Galloway, *Mar. Pollut. Bull.*, 2011, **62**, 2588.
5 V. Hidalgo-Ruz, L. Gutow, R. C. Thompson and M. Thiel, *Environ. Sci. Technol.*, 2012, **46**, 3060.
6 US Geological Survey, *Sulfur Production Worldwide in 2022, by Country*, Statista, 2023, retrieved December 27, 2023, from **https://www-statista-com.libproxy.clemson.edu/statistics/1031181/sulfur-production-globally-by-country/**.
7 A. Tanimu and K. Alhooshani, *Energy Fuels*, 2019, **33**, 2810.
8 W. J. Chung, J. J. Griebel, E. T. Kim, H. Yoon, A. G. Simmonds, H. J. Ji, P. T. Dirlam, R. S. Glass, J. J. Wie, N. A. Nguyen, B. W. Guralnick, J. Park, A. Somogyi, P. Theato, M. E. Mackay, Y.-E. Sung, K. Char and J. Pyun, *Nat. Chem.*, 2013, **5**, 518.
9 J. Bao, K. P. Martin, E. Cho, K.-S. Kang, R. S. Glass, V. Coropceanu, J.-L. Bredas, W. O. N. Parker Jr, J. T. Njardarson and J. Pyun, *J. Am. Chem. Soc.*, 2023, **145**, 12386.
10 J. J. Griebel, R. S. Glass, K. Char and J. Pyun, *Prog. Polym. Sci.*, 2016, **58**, 90.
11 J. Lim, J. Pyun and K. Char, *Angew. Chem., Int. Ed.*, 2015, **54**, 3249.
12 J. J. Griebel, N. A. Nguyen, S. Namnabat, L. E. Anderson, R. S. Glass, R. A. Norwood, M. E. MacKay, K. Char and J. Pyun, *ACS Macro Lett.*, 2015, **4**, 862.
13 W. J. Chung, J. J. Griebel, E. T. Kim, H. Yoon, A. G. Simmonds, H. J. Ji, P. T. Dirlam, R. S. Glass, J. J. Wie, N. A. Nguyen, B. W. Guralnick, J. Park, Á. Somogyi,

P. Theato, M. E. Mackay, Y.-E. Sung, K. Char and J. Pyun, *Nat. Chem.*, 2013, **5**, 518.
14 J. M. Chalker, M. J. H. Worthington, N. A. Lundquist and L. J. Esdaile, *Top. Curr. Chem.*, 2019, **377**, 16.
15 A. Gupta, M. J. H. Worthington, H. D. Patel, M. R. Johnston, M. Puri and J. M. Chalker, *ACS Sustain. Chem. Eng.*, 2022, **10**, 9022.
16 N. A. Lundquist, A. D. Tikoalu, M. J. H. Worthington, R. Shapter, S. J. Tonkin, F. Stojcevski, M. Mann, C. T. Gibson, J. R. Gascooke, A. Karton, L. C. Henderson, L. J. Esdaile and J. M. Chalker, *Chem.–Eur. J.*, 2020, **26**, 10035.
17 P. Yan, W. Zhao, S. J. Tonkin, J. M. Chalker, T. L. Schiller and T. Hasell, *Chem. Mater.*, 2022, **34**, 1167.
18 I. Bu Najmah, N. A. Lundquist, M. K. Stanfield, F. Stojcevski, J. A. Campbell, L. J. Esdaile, C. T. Gibson, D. A. Lewis, L. C. Henderson, T. Hasell and J. M. Chalker, *ChemSusChem*, 2021, **14**, 2352.
19 J. M. Chalker, M. Mann, M. J. H. Worthington and L. J. Esdaile, *Org. Mater.*, 2021, **03**, 362.
20 B. Zhang, H. Gao, P. Yan, S. Petcher and T. Hasell, *Mater. Chem. Front.*, 2020, **4**, 669.
21 J. A. Smith, R. Mulhall, S. Goodman, G. Fleming, H. Allison, R. Raval and T. Hasell, *ACS Omega*, 2020, **5**, 5229.
22 J. A. Smith, X. Wu, N. G. Berry and T. Hasell, *J. Polym. Sci., Part A: Polym. Chem.*, 2018, **56**, 1777.
23 D. J. Parker, S. T. Chong and T. Hasell, *RSC Adv.*, 2018, **8**, 27892.
24 K. B. Sayer, V. L. Miller, Z. Merrill, A. E. Davis and C. L. Jenkins, *Polym. Chem.*, 2023, **14**, 3091.
25 A. E. Davis, K. B. Sayer and C. L. Jenkins, *Polym. Chem.*, 2022, **13**, 4634.
26 C. R. Westerman and C. L. Jenkins, *Macromolecules*, 2018, **51**, 7233.
27 J. Dunn and C. L. Jenkins, *Nat. Synth.*, 2022, **1**, 835.
28 C. Herrera, K. J. Ysinga and C. L. Jenkins, *ACS Appl. Mater. Interfaces*, 2019, **11**, 35312.
29 C. R. Westerman, P. M. Walker and C. L. Jenkins, *J. Visualized Exp.*, 2019, e59620.
30 K. Orme, A. H. Fistrovich and C. L. Jenkins, *Macromolecules*, 2020, **53**, 9353.
31 M. L. Eder, C. B. Call and C. L. Jenkins, *ACS Appl. Polym. Mater.*, 2022, **4**, 1110.
32 S. Diez, A. Hoefling, P. Theato and W. Pauer, Mechanical and Electrical Properties of Sulfur-Containing Polymeric Materials Prepared via Inverse Vulcanization, *Polymers*, 2017, **9**, 59.
33 H. Mutlu, E. B. Ceper, X. Li, J. Yang, W. Dong, M. M. Ozmen and P. Theato, *Macromol. Rapid Commun.*, 2019, **40**, 1800650.
34 M. E. Duarte, B. Huber, P. Theato and H. Mutlu, *Polym. Chem.*, 2020, **11**, 241.
35 I. Gomez, O. Leonet, J. A. Blazquez and D. Mecerreyes, *ChemSusChem*, 2016, **9**, 3419.
36 I. Gomez, D. Mecerreyes, J. A. Blazquez, O. Leonet, H. Ben Youcef, C. Li, J. L. Gómez-Cámer, O. Bondarchuk and L. Rodriguez-Martinez, *J. Power Sources*, 2016, **329**, 72.
37 I. Gomez, O. Leonet, J. Alberto Blazquez, H.-J. Grande and D. Mecerreyes, *ACS Macro Lett.*, 2018, **7**, 419.
38 I. Gomez, A. F. De Anastro, O. Leonet, J. A. Blazquez, H.-J. Grande, J. Pyun and D. Mecerreyes, *Macromol. Rapid Commun.*, 2018, **39**, 1800529.
39 M. S. Karunarathna, M. K. Lauer, A. G. Tennyson and R. C. Smith, *Polym. Chem.*, 2020, **11**, 1621.
40 C. V. Lopez, C. P. Maladeniya and R. C. Smith, Lithium-Sulfur Batteries: Advances and Trends, *Electrochem*, 2020, **1**, 226.
41 M. S. Karunarathna, M. K. Lauer and R. C. Smith, *J. Mater. Chem. A*, 2020, **8**, 20318.
42 C. V. Lopez, A. D. Smith and R. C. Smith, *RSC Adv.*, 2022, **12**, 1535.
43 M. K. Lauer, A. G. Tennyson and R. C. Smith, *Mater. Adv.*, 2021, **2**, 2391.
44 A. D. Smith, A. G. Tennyson and R. C. Smith, Sulfur-Containing Polymers Prepared from Fatty Acid-Derived Monomers: Application of Atom-Economical Thiol-ene/Thiol-yne Click Reactions and Inverse Vulcanization Strategies, *Sustainable Chem.*, 2020, **1**, 209.
45 M. K. Lauer, T. A. Estrada-Mendoza, C. D. McMillen, G. Chumanov, A. G. Tennyson and R. C. Smith, *Adv. Sustainable Syst.*, 2019, **3**, 1900062.
46 M. K. Lauer, A. G. Tennyson and R. C. Smith, *ACS Appl. Polym. Mater.*, 2020, **2**, 3761.
47 A. D. Smith, T. Thiounn, E. W. Lyles, E. K. Kibler, R. C. Smith and A. G. Tennyson, *J. Polym. Sci., Part A:Polym. Chem.*, 2019, **57**, 1704.
48 A. D. Smith, C. D. McMillin, R. C. Smith and A. G. Tennyson, *J. Polym. Sci.*, 2020, **58**, 438.
49 C. V. Lopez, M. S. Karunarathna, M. K. Lauer, C. P. Maladeniya, T. Thiounn, E. D. Ackley and R. C. Smith, *J. Polym. Sci.*, 2020, **58**, 2259.
50 C. P. Maladeniya, M. S. Karunarathna, M. K. Lauer, C. V. Lopez, T. Thiounn and R. C. Smith, *Mater. Adv.*, 2020, **1**, 1665.
51 C. P. Maladeniya, N. L. K. Dona, A. D. Smith and R. C. Smith, *Macromol*, 2023, **3**, 681.
52 M. K. Lauer, M. S. Karunarathna, A. G. Tennyson and R. C. Smith, *Materials Advances*, 2020, **1**, 590.
53 M. K. Lauer, M. S. Karunarathna, A. G. Tennyson and R. C. Smith, *Materials Advances*, 2020, **1**, 2271.
54 M. K. Lauer, Z. E. Sanders, A. D. Smith and R. C. Smith, *Mater. Adv.*, 2021, **2**, 7413.
55 B. G. S. Guinati, P. Y. Sauceda Oloño, N. L. Kapuge Dona, K. M. Derr, S. K. Wijeyatunga, A. G. Tennyson and R. C. Smith, *RSC Sustainability*, 2024, **2**, 1819–1827.
56 C. P. Maladeniya, A. G. Tennyson and R. C. Smith, *J. Polym. Sci.*, 2023, **61**, 787.
57 K. M. Derr, C. V. Lopez, C. P. Maladeniya, A. G. Tennyson and R. C. Smith, *J. Polym. Sci.*, 2023, **61**, 3075.
58 M. K. Lauer, M. S. Karunarathna, A. G. Tennyson and R. C. Smith, *Materials Advances*, 2020, **1**, 590.
59 K. M. Derr and R. C. Smith, Thiocracking of Multi-Materials: High-Strength Composites from Post-Consumer Food Packaging Jars, *Sustainability*, 2024, **16**, 7023.
60 S. K. Wijeyatunga, A. G. Tennyson and R. C. Smith, *ACS Sustainable Resour. Manage.*, 2024, **1**, 2173.

61 S. K. Wijeyatunga, K. M. Derr, C. P. Maladeniya, P. Y. Sauceda-Oloño, A. G. Tennyson and R. C. Smith, *J. Polym. Sci.*, 2024, **62**, 554.
62 K. M. Derr and R. C. Smith, *J. Polym. Sci.*, 2023, **62**, 1115.
63 R. A. Sheldon, *Green Chem.*, 2007, **9**, 1273.
64 B. G. S. Guinati, P. Y. Sauceda Oloño, N. L. Kapuge Dona, K. M. Derr, S. K. Wijeyatunga, A. G. Tennyson and R. C. Smith, *RSC Sustainability*, 2024, **2**, 1819.
65 J. J. Dale, S. Petcher and T. Hasell, *ACS Appl. Polym. Mater.*, 2022, **4**, 3169.
66 J. J. Dale, J. Stanley, R. A. Dop, G. Chronowska-Bojczuk, A. J. Fielding, D. R. Neill and T. Hasell, *Eur. Polym. J.*, 2023, **195**, 112198.
67 ACI Committee 332, *Guide to Residential Concrete Construction*, ACI 332.1R-06, American Concrete Institute, Farmington Hills, MI, 2006.
68 M. H. Riaz, A. Khitab, S. Ahmad, W. Anwar and M. T. Arshad, *Asian Journal of Civil Engineering*, 2020, **21**, 243.
69 T. V. T. Phan, C. Gallardo and J. Mane, *Green Chem.*, 2015, **17**, 2846.
70 A. Dormer, D. P. Finn, P. Ward and J. Cullen, *J. Cleaner Prod.*, 2013, **51**, 133.
71 L. K. Turner and F. G. Collins, *Constr. Build. Mater.*, 2013, **43**, 125.
72 K. E. Tomberlin, R. Venditti and Y. Yao, *BioResources*, 2020, **15**, 3899.
73 W. Russ and R. Meyer-Pittroff, *Crit. Rev. Food Sci. Nutr.*, 2004, **44**, 57.
74 L. K. Brogaard, A. Damgaard, M. B. Jensen, M. Barlaz and T. H. Christensen, *Resour., Conserv. Recycl.*, 2014, **87**, 30.
75 U. Arena and F. Ardolino, *Resour., Conserv. Recycl.*, 2022, **183**, 106379.
76 H. Jeswani, C. Krüger, M. Russ, M. Horlacher, F. Antony, S. Hann and A. Azapagic, *Sci. Total Environ.*, 2021, **769**, 144483.
77 F. Passarini, L. Ciacci, A. Santini, I. Vassura and L. Morselli, *J. Cleaner Prod.*, 2012, **23**, 28.
78 W. Peukert, *Int. J. Miner. Process.*, 2004, **74**, S3.
79 G. Schubert and S. Bernotat, *Int. J. Miner. Process.*, 2004, **74**, S19.
80 D. Wüstenberg and J. Kasper, *Int. J. Miner. Process.*, 2004, **74**, S417.
81 F. G. Müller, L. S. Lisboa and J. M. Chalker, *Adv. Sustainable Syst.*, 2023, **7**, 2300010.
82 M. J. H. Worthington, R. L. Kucera and J. M. Chalker, *Green Chem.*, 2017, **19**, 2748.
83 T. Lee, P. T. Dirlam, J. T. Njardarson, R. S. Glass and J. Pyun, *J. Am. Chem. Soc.*, 2022, **144**, 5.
84 Y. Zhang, R. S. Glass, K. Char and J. Pyun, *Polym. Chem.*, 2019, **10**, 4078.
85 J. Bao, K. P. Martin, E. Cho, K.-S. Kang, R. S. Glass, V. Coropceanu, J.-L. Bredas, W. O. N. Parker Jr, J. T. Njardarson and J. Pyun, *J. Am. Chem. Soc.*, 2023, **145**, 12386.
86 A. Amin, N. M. Mahmoud and Y. W. Z. Nisa, *Green Mater.*, 2020, **8**, 172.
87 G. N. Lewis and M. Randall, *J. Am. Chem. Soc.*, 1911, **33**, 476.